LONG-PERIOD RAYLEIGH WAVE SPECTRA FROM EARTHQUAKES AND EXPLOSIONS

S. S. Alexander, et al

Teledyne Geotech

Prepared for:

Air Force Technical Applications Center
Advanced Research Projects Agency

2 March 1973

307

LONG-PERIOD RAYLEIGH WAVE SPECTRA FROM EARTHQUAKES AND EXPLOSIONS

S.S. ALEXANDER
CONSULTANT TO THE SEISMIC DATA LABORATORY

J.W. LAMBERT
SEISMIC DATA LABORATORY

2 MARCH 1973

Prepared for
AIR FORCE TECHNICAL APPLICATIONS CENTER
Washington, D.C.

Under
Project VELA UNIFORM

Sponsored by
ADVANCED RESEARCH PROJECTS AGENCY
Nuclear Monitoring Research Office
ARPA Order No. 1714

TELEDYNE GEOTECH
ALEXANDRIA LABORATORIES

39

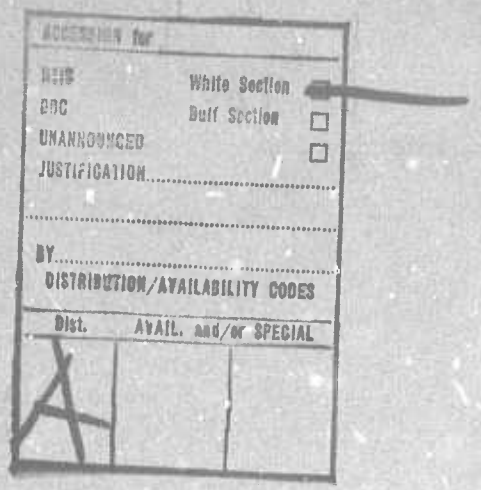

Unclassified
Security Classification

DOCUMENT CONTROL DATA - R&D

(Security classification of title, body of abstract and indexing annotation must be entered when the overall report is classified)

1. ORIGINATING ACTIVITY (Corporate author) Teledyne Geotech Alexandria, Virginia 22314	2a. REPORT SECURITY CLASSIFICATION Unclassified 2b GROUP

3 REPORT TITLE

LONG-PERIOD RAYLEIGH WAVE SPECTRA FROM EARTHQUAKES AND EXPLOSIONS

4. DESCRIPTIVE NOTES (Type of report and inclusive dates)

Scientific

5. AUTHOR(S) (Last name, first name, initial)

Alexander, S.S.; Lambert, J.W.

6. REPORT DATE 2 March 1973	7a. TOTAL NO. OF PAGES ~~31~~ 39	7b. NO. OF REFS 6
8a. CONTRACT OR GRANT NO. F33657-72-C-0009 b. PROJECT NO. VELA T/2706 c. ARPA Order No. 1714 dARPA Program Code No. 2F-10	9a. ORIGINATOR'S REPORT NUMBER(S) 307 9b. OTHER REPORT NO(S) (Any other numbers that may be assigned this report)	

10. AVAILABILITY/LIMITATION NOTICES

APPROVED FOR PUBLIC RELEASE; DISTRIBUTION UNLIMITED.

11. SUPPLEMENTARY NOTES	12. SPONSORING MILITARY ACTIVITY Advanced Research Projects Agency Nuclear Monitoring Research Office Washington, D.C.

13 ABSTRACT

Comparisons are made of Rayleigh wave spectra for NTS explosions and Nevada earthquakes and for a limited number of teleseismic explosions and earthquakes recorded in North America. For a given combination of source and receiver location, the explosions consistently exhibit the same spectral shape over a significant range of magnitudes while spectral shapes for earthquakes commonly vary in a manner that appears independent of magnitude, with some earthquake shapes closely matching those of explosions. The spectral shapes for explosions were commonly observed to vary significantly from station to station at comparable distance ranges, probably because of path and receiver site effects. We conclude that neither Rayleigh spectral shape nor symmetry of raw surface wave radiation patterns is likely to be a reliable discriminant in general.

14 KEY WORDS

Spectra
Rayleigh
Long-Period
Explosion
Earthquakes

Unclassified
Security Classification

LONG-PERIOD RAYLEIGH WAVE SPECTRA FROM EARTHQUAKES AND EXPLOSIONS

SEISMIC DATA LABORATORY REPORT NO. 307

AFTAC Project No.:	VELA T/2706
Project Title:	Seismic Data Laboratory
ARPA Order No.:	1714
ARPA Program Code No.:	2F-10
Name of Contractor:	TELEDYNE GEOTECH
Contract No.:	F33657-72-C-0009
Date of Contract:	01 July 1971
Amount of Contract:	$2,482,460
Contract Expiration Date:	30 June 1973
Project Manager:	Robert R. Blandford (703) 836-3882

P. O. Box 334, Alexandria, Virginia 22314

ABSTRACT

Comparisons are made of Rayleigh wave spectra for NTS explosions and Nevada earthquakes and for a limited number of teleseismic explosions and earthquakes recorded in North America. For a given combination of source and receiver location, the explosions consistently exhibit the same spectral shape over a significant range of magnitudes while spectral shapes for earthquakes commonly vary in a manner that appears independent of magnitude, with some earthquake shapes closely matching those of explosions. The spectral shapes for explosions were commonly observed to vary significantly from station to station at comparable distance ranges, probably because of path and receiver site effects. We conclude that neither Rayleigh spectral shape nor symmetry of raw surface wave radiation patterns is likely to be a reliable discriminant in general.

TABLE OF CONTENTS

TABLE TITLE

LIST OF FIGURES

LIST OF FIGURES (Cont'd.)

LIST OF FIGURES (Cont'd.)

INTRODUCTION

Because the relative excitation of Rayleigh waves and P waves as reflected even in simple M_s vs m_b relationships constitutes the basis for one of the most powerful seismic discriminants, it is important to examine the variability of the spectral excitation to be expected for earthquakes and explosions. Spectral shape (spectral splitting) and symmetry of Rayleigh wave radiation patterns have also been suggested as further diagnostic aids. In the following discussion of these criteria, spectra will be presented for Nevada earthquakes and explosions observed at regional and near-regional distances as well as spectra for a limited number of teleseismic explosions and earthquakes.

Table I gives the pertinent epicentral information and magnitude estimates for all the earthquakes and explosions used in this study. Figure 1 shows the composite M_s vs m_b plot for the entire data set of Table I. The body wave magnitudes are NOS values and the M_s values include the standard Gutenberg distance correction. Figure 2 shows M_s vs m_b data for the subset of Nevada earthquakes and NTS explosions for which adjusted M_s and m_b values are available. In this plot the adjusted m_b values have been determined using Evernden's empirical distance corrections for stations at regional (non-teleseismic) distances (Evernden, 1967) and the adjusted M_s values include von Seggern's distance correction factors for stations at less than 15° distance (von Seggern, 1970). The lines shown are the mean

M_s vs m_b curves for Nevada earthquakes and NTS explosions, and the best discriminant line separating the two populations as given by Lambert and Alexander (1971) for larger data sets of explosions and earthquakes in Nevada.

RESULTS

Figures 3 and 4 show nuclear explosion spectra and Nevada earthquake spectra at BMO, which is at an epicentral distance of between 860 and 881 km for all events. The explosion spectra are very similar in shape (except for PAR, which was a small event with a poor signal-to-noise ratio over the entire frequency band considered). The earthquake spectra shown in Figure 4 are from events within a local source region (as indicated in Table I). Their spectra are less consistent than those for the explosion, showing a double-peaked structure and no systematic change with magnitude. Note that spectral splitting would not work well on these spectra unless the spectral windows are carefully selected.

Figure 5 shows explosion spectra for UBO at a distance of around 665 km. Again there is general consistency among events but the spectral shape at UBO is distinctly different than for the same events observed at BMO (Figure 3) or TFO (Figure 8), indicating a strong effect of propagation path and site response on the Rayleigh wave spectra.

Note in this connection that even though TFO is more than 300 km closer to the source than BMO, the spectral peak at TFO occurs at a lower frequency (.05 - .06 Hz vs .06 - .07 Hz) for the same set of events. The spectra at HL-ID (Figure 6) at 738 km distance are peaked at a still higher frequency (~.07 Hz) whereas the spectrum at LC-NM (Figure 7), at ~1000 km

distance, peaks between .05 and .06 Hz. It appears from these data that the higher frequencies are more rapidly attenuated toward the southeast from NTS than toward the north. Although asymmetry in radiation of energy from the source may account for some of this variation, the similarity in spectral shape from shot to shot for differing yields argues against the variations being due primarily to a source effect.

In Figures 8 and 9 we compare explosions and earthquakes at TFO in the distance range of 427-543 km. Again there is consistency for the explosions but not for the earthquakes.

Figure 10 from Evernden et al. (1971) shows still another example of the similarity of explosion spectral shapes for Rayleigh waves when the path from source to receiver is nearly the same. The events shown were all located on Pahute Mesa and were recorded at Berkley, California. At higher frequencies even the detailed shape of the observed spectra is replicated from event to event, including that of PIPKIN which was about .8 magnitude units smaller than the others (Table I).

Overall, these data suggest that the Rayleigh wave spectra of explosions for a given source region-station combination can be expected to remain similar to one another for all events, while the earthquake spectra can vary significantly in shape at any magnitude, with some being similar to the explosions. This general lack of similarity for earthquake spectra is to be expected if the events have different source parameters (e.g. fault strike, dip, slip, depth), as von Seggern (1969, 1970)

has pointed out. This result implies that spectral shape in general may not be a very reliable discriminant between earthquakes and explosions, although it possibly could be used to identify some earthquakes if the spectral shapes observed are dissimilar enough from those of explosions from a given source region. On the other hand, it should be noted that even though spectral shapes might coincide for earthquakes and explosions, observed M_s vs m_b data imply that the Rayleigh excitation level for a given m_b event averaged over azimuth will be greater for an earthquake than for an explosion (Figure 2). The danger is, of course, that with only a few stations or with poor azimuthal coverage, radiation patterns and similar spectral shapes may combine to give low Rayleigh wave signal levels for earthquakes at all the available stations, thereby causing the earthquake to be mistaken for an explosion.

In Figures 11 and 12 we compare the spectra of three teleseismic events recorded at KN-UT and LC-NM. The observed spectral shapes are very dissimilar at KN-UT (Figure 11), while two of the same events are similar at LC-NM. These differences result from a combination of path and source effects that cannot easily be separated. In any case, we conclude that earthquakes from the Kamchatka area do not seem to have consistent Rayleigh wave spectral shapes from event to event. Also, there is no systematic variation of spectral shape with magnitude; again this is to be expected because of the dominant influence of fault parameters on spectral shape of earthquakes (von Seggern 1969, 1970).

In Figures 13 through 18 we compare the LONG SHOT and MILROW spectra recorded at different LRSM stations with spectra from various earthquakes of comparable magnitudes located in the same source region. It is important to note that LONG SHOT and MILROW consistently have the same spectral shape at each station, although there are significant variations in shape from station to station due principally to propagation and site effects.

Compare KN-UT (Figure 16), PG-BC (Figure 17) and RK-ON (Figure 18), for example. The earthquakes show no consistent pattern, some being similar at a given station (presumably implying a similar source mechanism) and others being significantly different in spectral shape. RK-ON (Figure 18) is an example where the explosion spectrum peaks at a considerably lower frequency than earthquakes of comparable magnitude from the same region, which means that spectral splitting would fail as a diagnostic in this instance. Since for each station the source region is the same, assuring that path effects are in common for these events, the spectral differences observed must represent actual differences in source mechanism for the earthquakes.

Because the observed spectral shapes of explosions have been shown to differ from station to station at comparable distance ranges but at different azimuths, this will appear as a frequency-dependent radiation pattern, which is normally indicative of an earthquake type of source mechanism (von Seggern and Lambert 1969). Thus we conclude that path and site effects must be

properly accounted for before radiation patterns of Rayleigh waves can be used as diagnostic aids to identify explosions. One way this problem can be overcome is to use a reference event approach whereby the spectra are normalized by the observed spectrum of a well-documented reference event from the same source region, so that transmission effects are cancelled.

CONCLUSIONS

1. For a given combination of source region and station location, explosion spectra were observed consistently to have the same spectral shape even for different magnitude events.

2. Spectral shapes observed for explosions commonly vary significantly from station to station at comparable distances due to path and site effects; in turn this produces an apparent radiation pattern that is not associated with the source.

3. Earthquake spectra at given stations commonly vary in shape for different events of comparable magnitude within the same source region; this conforms to what is predicted theoretically.

4. Because the paths to individual stations were common for the cases investigated, the observed spectral differences for earthquakes indicate different source mechanisms for events within the same source region at NTS, in the Aleutians, and in Kamchatka.

5. There appears to be no consistent variation in Rayleigh wave spectral shape with magnitude (m_b) for earthquakes; this is in accordance with theoretical predictions for earthquake sources.

6. Spectral splitting at a single station is not likely to be a reliable discriminant, although events with spectra different from known explosion spectra possibly can be identified as earthquakes; however, positive identification of explosions may fail completely, because earthquakes were observed to produce

Rayleigh wave spectra with shapes closely matching those for explosions in the same source region.

7. Path and receiver site effects on the spectra must be properly accounted for before the frequency dependence of Rayleigh wave radiation patterns can be used as a diagnostic.

8. A reference event approach is recommended for spectral comparisons in order to eliminate propagation and site effects and to isolate source effects.

REFERENCES

Evernden, J.F., 1967, Magnitude determination at regional and near-regional distances in the United States: Bull. Seismol. Soc. Amer., v. 57, p. 591-639.

Evernden, J.F., Best, W.J., Pomeroy, P.W., McEvilly, T.V., Savino, J.M., and Sykes, L.R., 1971, Discrimination between small-magnitude earthquakes and explosions: J. Geophys. Res., v. 76, No. 32, p. 8042-8055.

Lambert, D.G. and Alexander, S.S., 1971, Relationship of body and surface-wave magnitudes for small earthquakes and explosions: Seismic Data Laboratory Report No. 245, Teledyne Geotech, Alexandria, Virginia.

von Seggern, D.H., 1969, Effects of radiation patterns on spectra and magnitude estimates: Seismic Data Laboratory Report No. 233, Teledyne Geotech, Alexandria, Virginia.

von Seggern, D.H., 1970, Surface wave amplitude versus distance relation in the Western United States: Seismic Data Laboratory Report No. 249, Teledyne Geotech, Alexandria, Virginia.

von Seggern, D.H. and Lambert, D.G., 1970, Theoretical and observed Rayleigh-wave spectra for explosions and earthquakes: J. Geophys. Res., v. 75, p. 7382-7402.

TABLE I

Magnitudes of Explosions and Earthquakes

DATE	EVENT AND NUMBERS	LOCATION	ORIGIN TIME	DEPTH Km	BODY-WAVE MAGNITUDE m_b(a)	adjusted	RAYLEIGH-WAVE MAGNITUDE M_s	adjusted	NUMBER OF STATIONS m_b(b)	M_s
24 Apr 64	TURF (1)	37°09.0'N 116°03.3'W	21 10 00.2	0.49	4.95	4.55	3.72	4.06	36	32
09 Oct 64	PAR (2)	37°09.1'N 116°04.6'W	14 00 00.1	0.92	4.78	4.44	2.55	3.13	32	17
26 Mar 65	CUP (3)	37°08.9'N 116°02.6'W	15 34 08.2	0.75	5.25	4.84	3.93	4.30	30	24
23 Jul 65	BRONZE (4)	37°05.9'N 116°02.0'W	17 00 00.0	0.53	5.22	4.87	4.14	4.50	31	28
03 Dec 65	CORDUROY (5)	37°09.9'N 116°03.0'W	15 13 02.1	0.68	5.62	5.42	4.53	4.77	28	21
06 Apr 66	STUTZ (6)	37°08.4'N 116°08.4'W	13 57 17.1	0.23	4.45	4.15	2.49	2.87	17	3
19 May 66	DUMONT (7)	37°06.7'N 116°03.5'W	13 56 28.1	0.67	5.48	5.27	4.47	4.69	22	18
20 Jan 67	BOURBON (8)	37°06.0'N 116°00.2'W	17 40 04.4	0.56	5.09	4.78	4.19	4.49	14	13
20 May 67	COMMODORE (9)	37°07.8'N 116°03.8'W	15 00 00.2	0.76	5.68	5.40	5.02	5.24	20	17
26 Apr 68	BOXCAR (10)	37°17.7'N 116°27.4'W	15 00 00.0	1.32	6.42	6.14	5.42	5.86	19	16
09 Dec 68	BENHAM (11)	37°13.9'N 116°28.6'W	16 30 00.0	1.40	6.40	5.89	5.52	5.72	6	8
16 Sep 69	JORUM (12)	37°18.8'N 116°27.6'W	14 30 00.0	1.16	6.2(c)		5.52		188	1
08 Oct 69	PIPKIN (13)	37°15.4'N 116°27.0'W	14 30 00.0	0.62	5.5(c)		4.23		95	1
17 Aug 66	S. Nevada (14)	37°24'N 114°06'W	23 07 58.9	33(d)	4.9(c)	4.15	3.90	4.27	13	12
18 Aug 66	S. Nevada (15)	37°18'N 114°12'W	09 15 37.5	33(d)	4.6(c)	4.14	4.05	4.31	15	16
18 Aug 66	S. Nevada (16)	37°24'N 114°12'W	17 35 06.4	33(d)	5. (c)	4.10	3.77	3.98	11	13
19 Aug 66	S. Nevada (17)	37°18'N 114°18'W	00 18 56.1	33(d)	4.7(c)		2.88		13	3
19 Aug 66	S. Nevada (18)	37°18'N 114°12'W	10 51 40.5	33(d)	4.2(c)	3.82	3.73	4.01	11	18
19 Aug 66	S. Nevada (19)	37°18'N 114°12'W	11 17 47.7	33(d)	4.4(c)	2.94	2.57	3.13	5	8
20 Aug 66	S. Nevada (20)	37°24'N 114°12'W	11 36 48.0	33(d)	4.2(c)		2.08		13	1
22 Aug 66	S. Nevada (21)	37°18'N 114°12'W	08 27 30.2	33(d)	4.8(c)	3.46	3.44	3.71	8	16
23 Sep 66	S. Nevada (22)	37°18'N 114°06'W	11 56 09.4	33(d)	4.5(c)		2.87		18	5
02 Oct 66	S. Nevada (23)	37°18'N 114°12'W	15 39 41.2	33(d)	4.5(c)		2.92		14	2
25 Oct 66	S. Nevada (24)	36°18'N 114°12'W	16 39 33.0	33(d)	4.4(c)		3.35		27	1
29 Oct 65	LONGSHOT (25)	51°26.3'N 179°11.0'E	21 00 00.1	0.70	5.85		4.21		180	31
02 Oct 69	MILROW (26)	51°25.0'N 179°10.9'E	22 06 00.1	1.22	6.42		4.84		51	47
29 Jan 65	Kamchatka (27)	54°48'N 161°42'E	09 35 25.7	33(d)	5.8(c)		4.86		34	16
14 Feb 65	Komandorsky (28)	55°06'N 165°36'E	17 01 13.9	20(d)	5.0(c)		3.99		16	13
20 Apr 65	Near Islands (29)	52°24'N 172°00'E	06 43 08.8	35(d)	5.5(c)		4.77		47	11
20 Apr 65	Kamchatka (30)	54°36'N 161°24'E	05 50 17.6	33(d)	5.3(c)		4.85		49	11
06 Nov 65	Rat Island (31)	51°18'N 172°42'E	22 30 16.6	40(d)	5.1(c)		4.33		32	15
22 Nov 65	Andreanoff Is.(32)	51°24'N 179°42'E	20 25 31.1	40(d)	5.86		5.56		90	9

(a) Unified m_b computed at SDL unless otherwise indicated.

(b) Recording stations used to compute adjusted magnitudes where adjusted magnitudes are shown

(c) NOS magnitudes.

(d) Constrained.

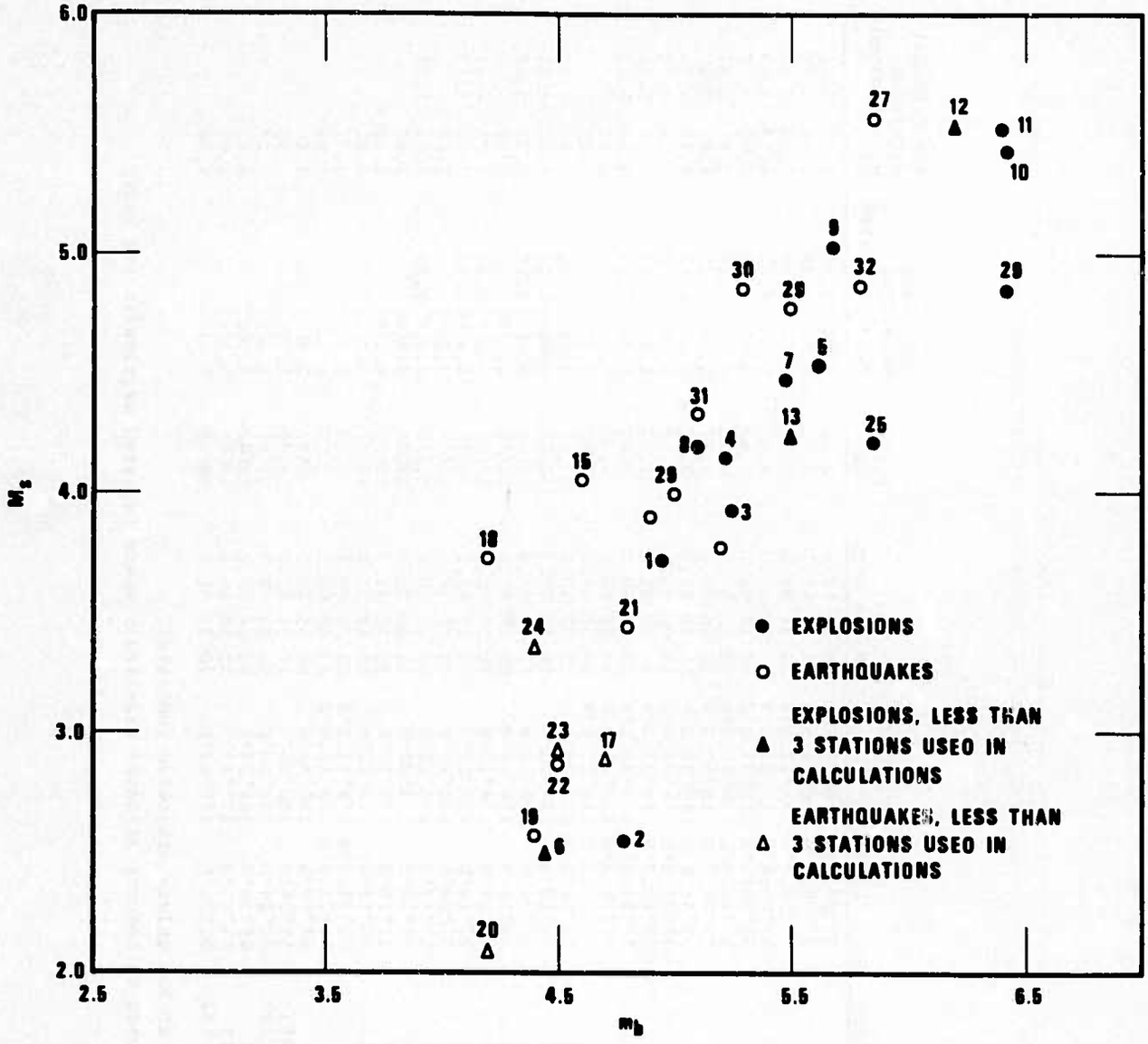

Figure 1. M_S (Gutenburg) vs unified m_b or m_b (NOS) for events used in this study. Event numbers refer to events listed in Table I.

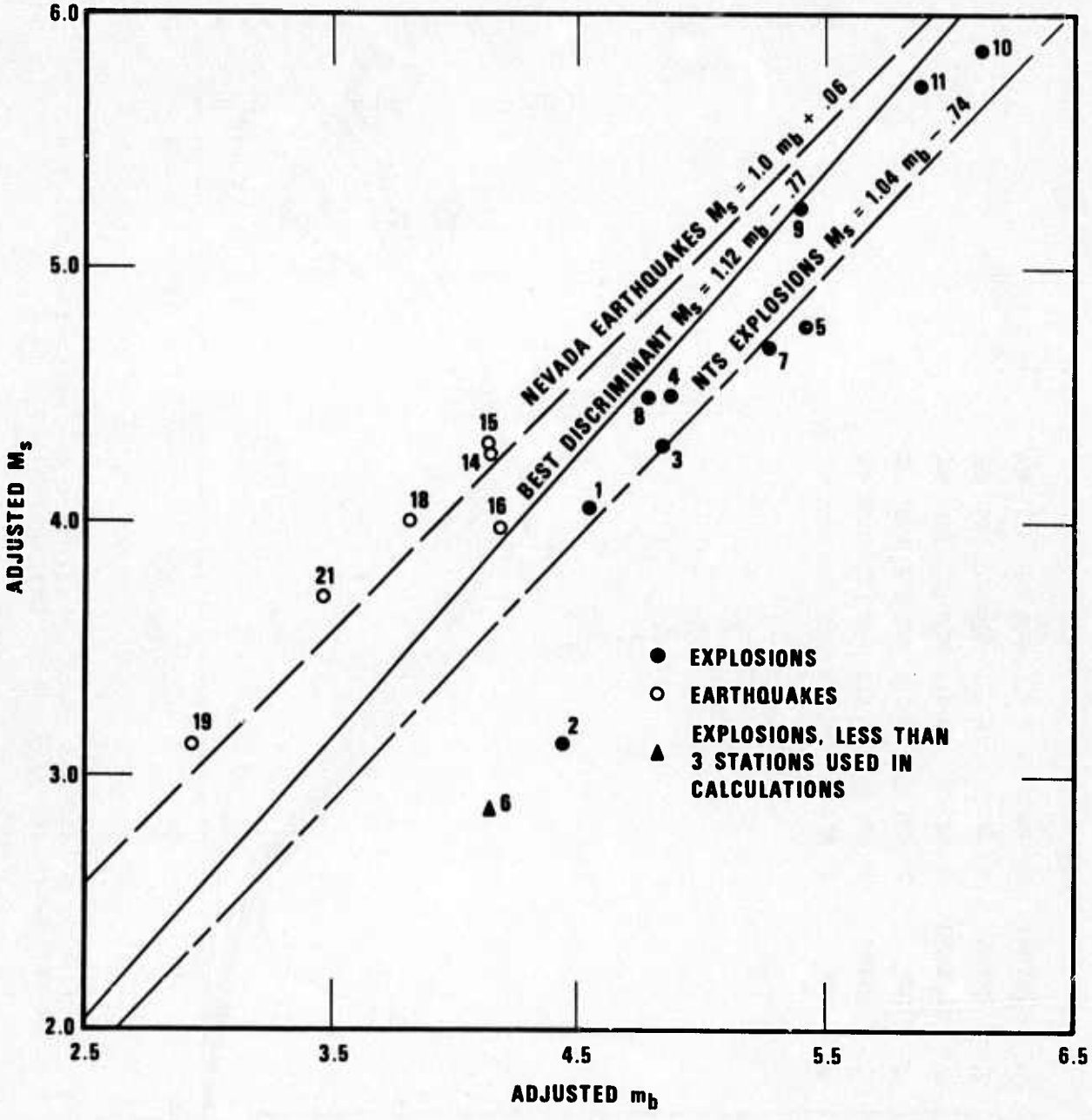

Figure 2. M_s adjusted vs m_b adjusted for a subset of Nevada earthquakes and NTS explosions given in Table I. Numbers refer to event numbers in Table I. Lines show mean curves and the best discriminant line for Nevada earthquakes and NTS explosions as determined by Lambert and Alexander (1971).

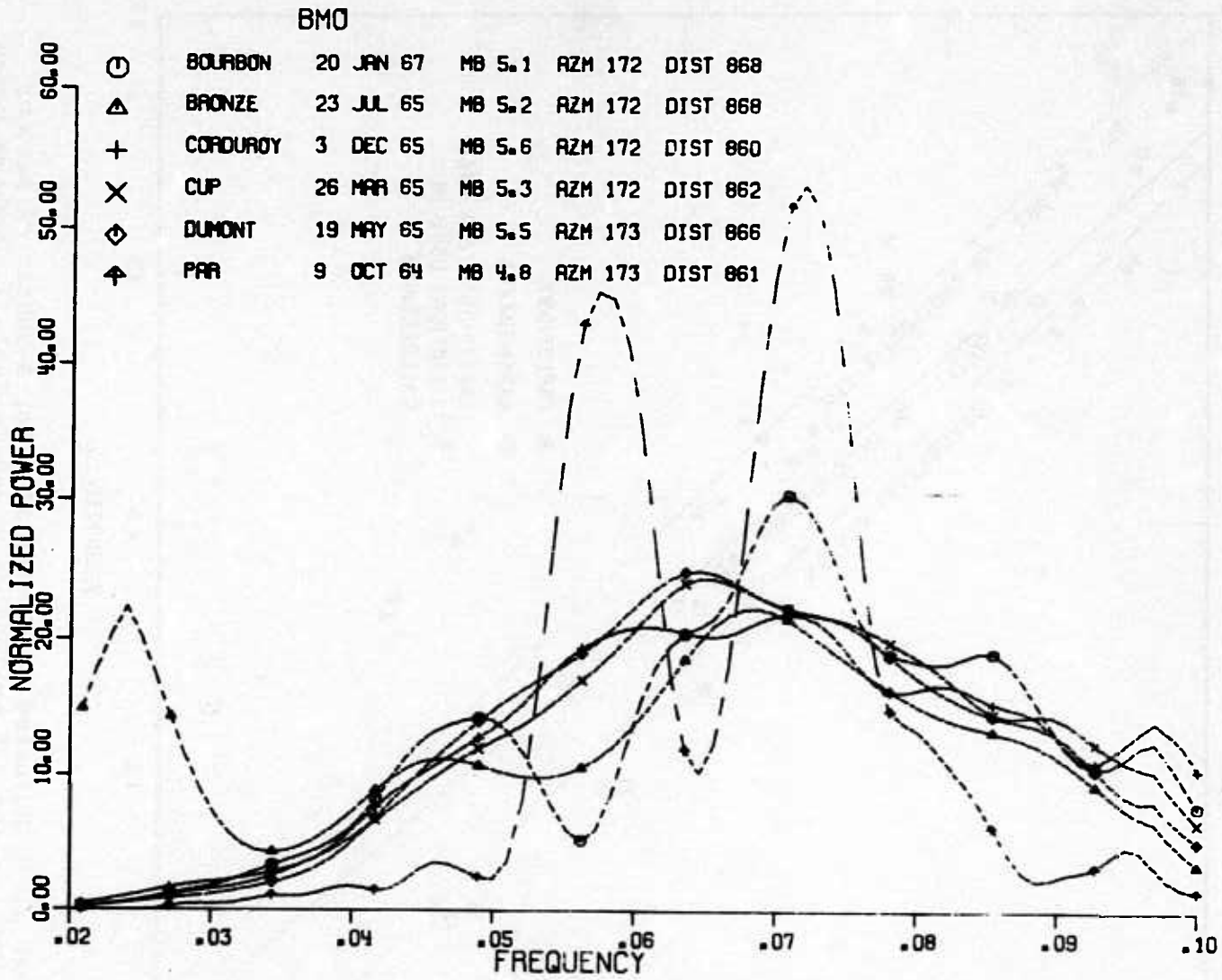

Figure 3. Normalized power spectra for NTS explosions observed at BMO (corrected for instrument response).

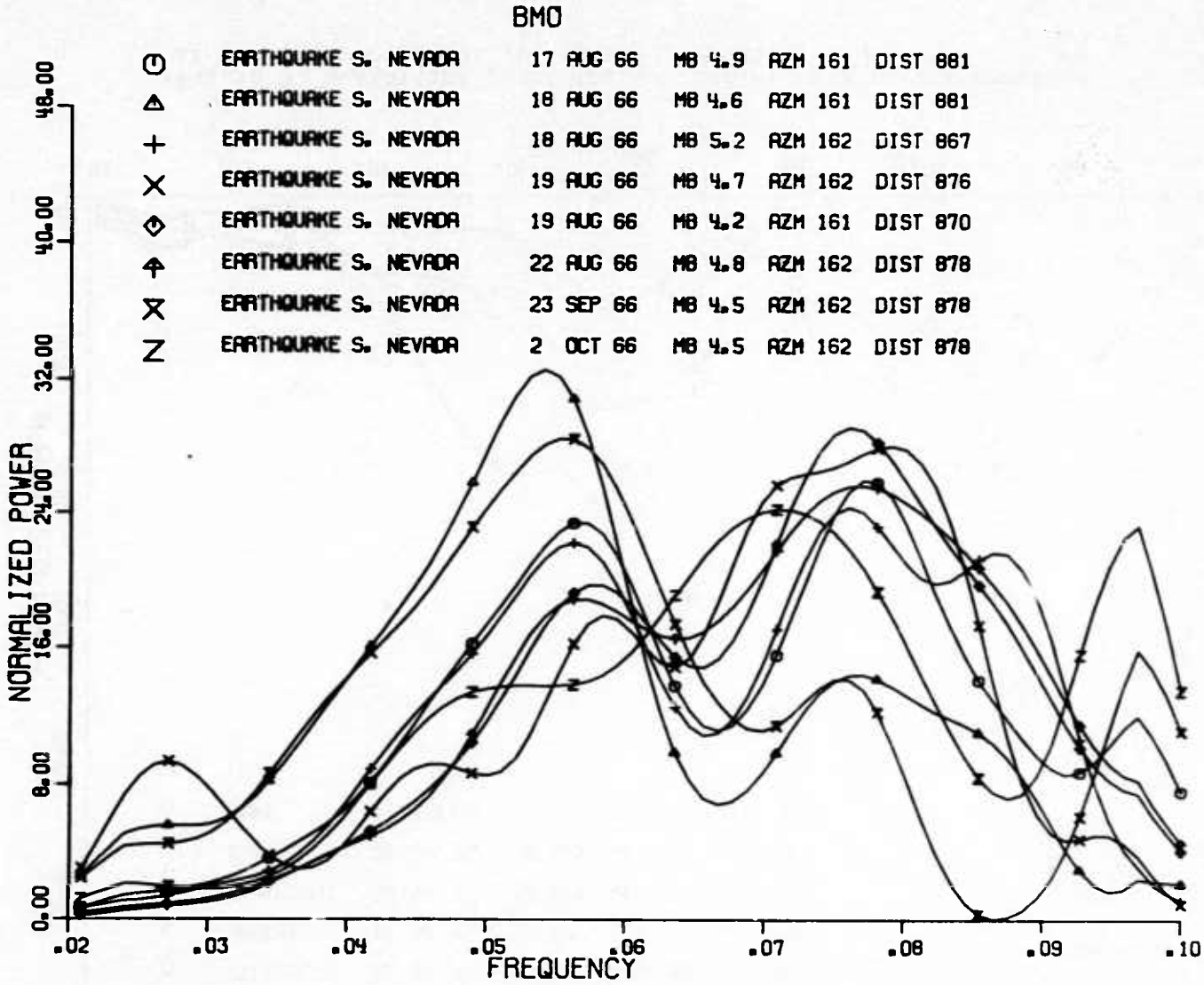

Figure 4. Normalized power spectra for Nevada earthquakes at BMO (corrected for instrument response).

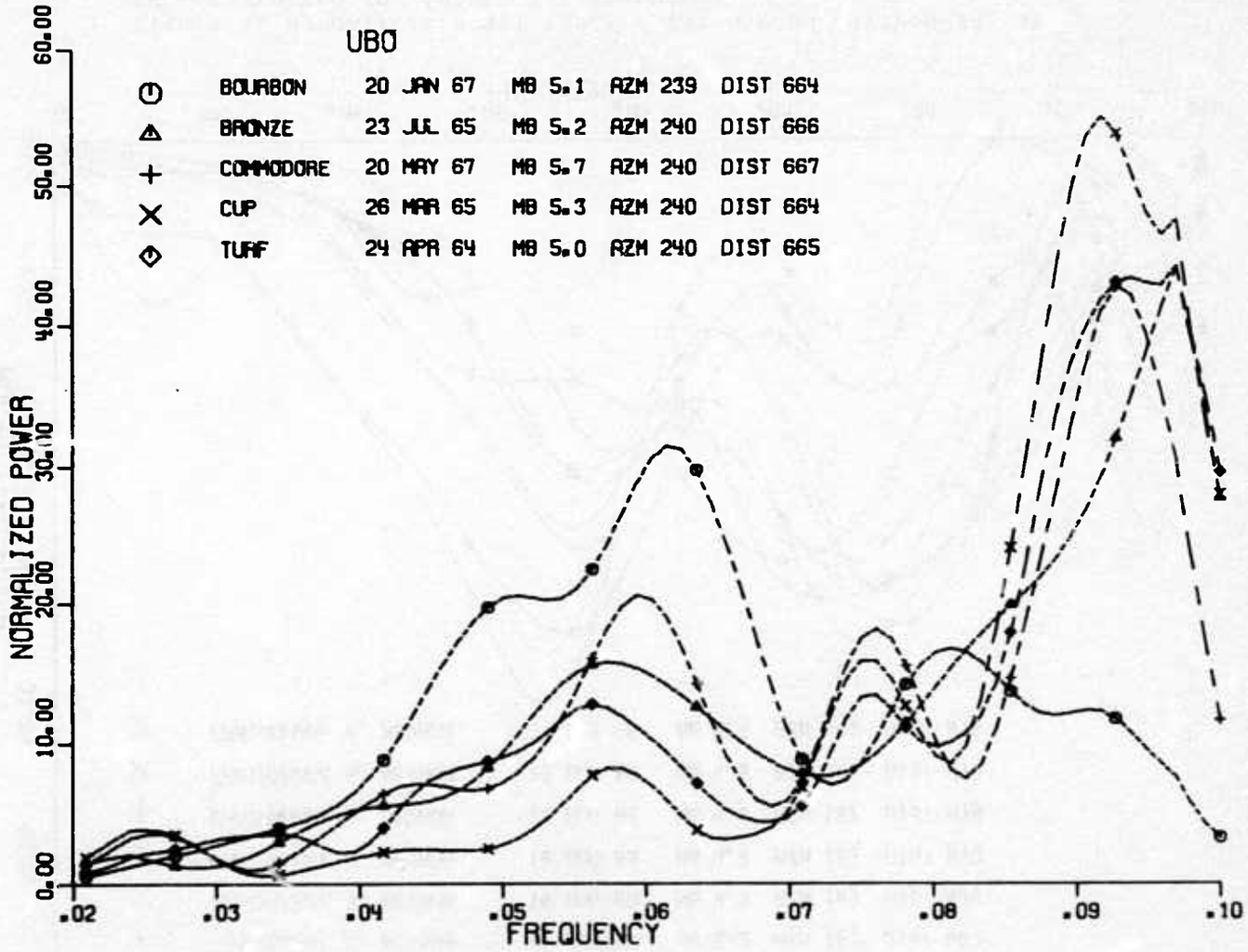

Figure 5. Normalized power spectra for NTS explosions observed at UBO (corrected for instrument response).

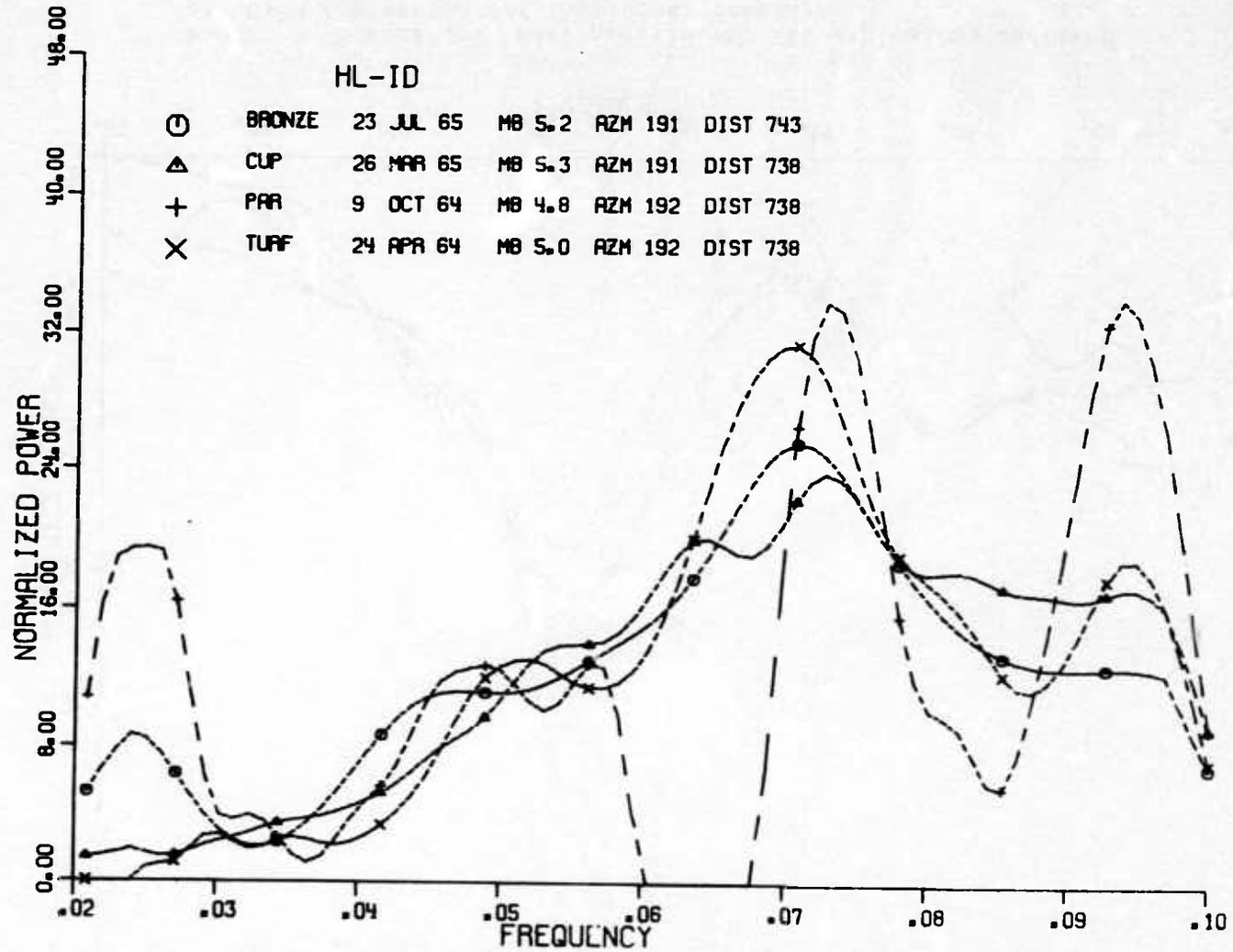

Figure 6. Normalized power spectra for NTS explosions observed at HL-ID (corrected for instrument response).

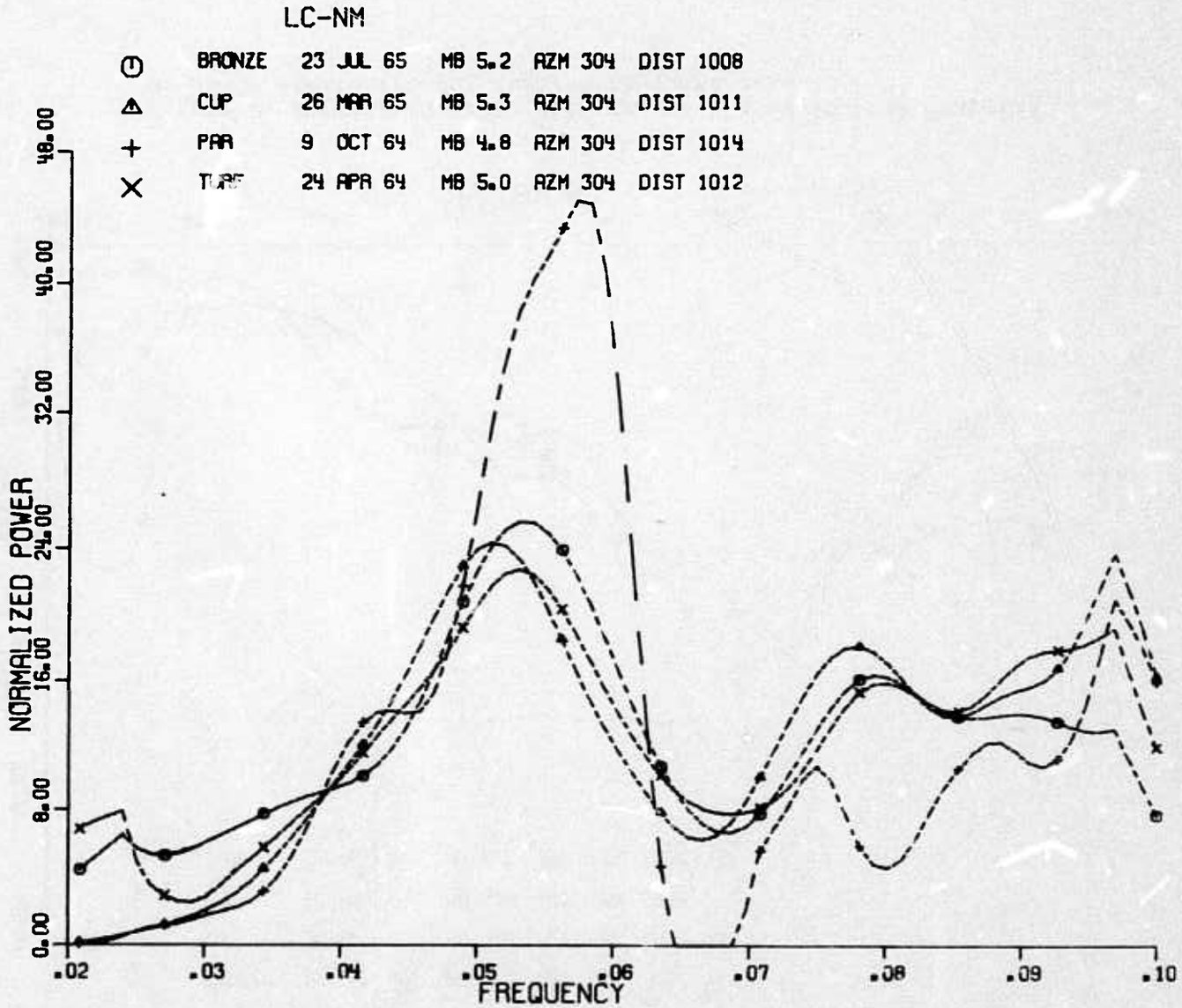

Figure 7. Normalized power spectra for NTS explosions observed at LC-NM (corrected for instrument response).

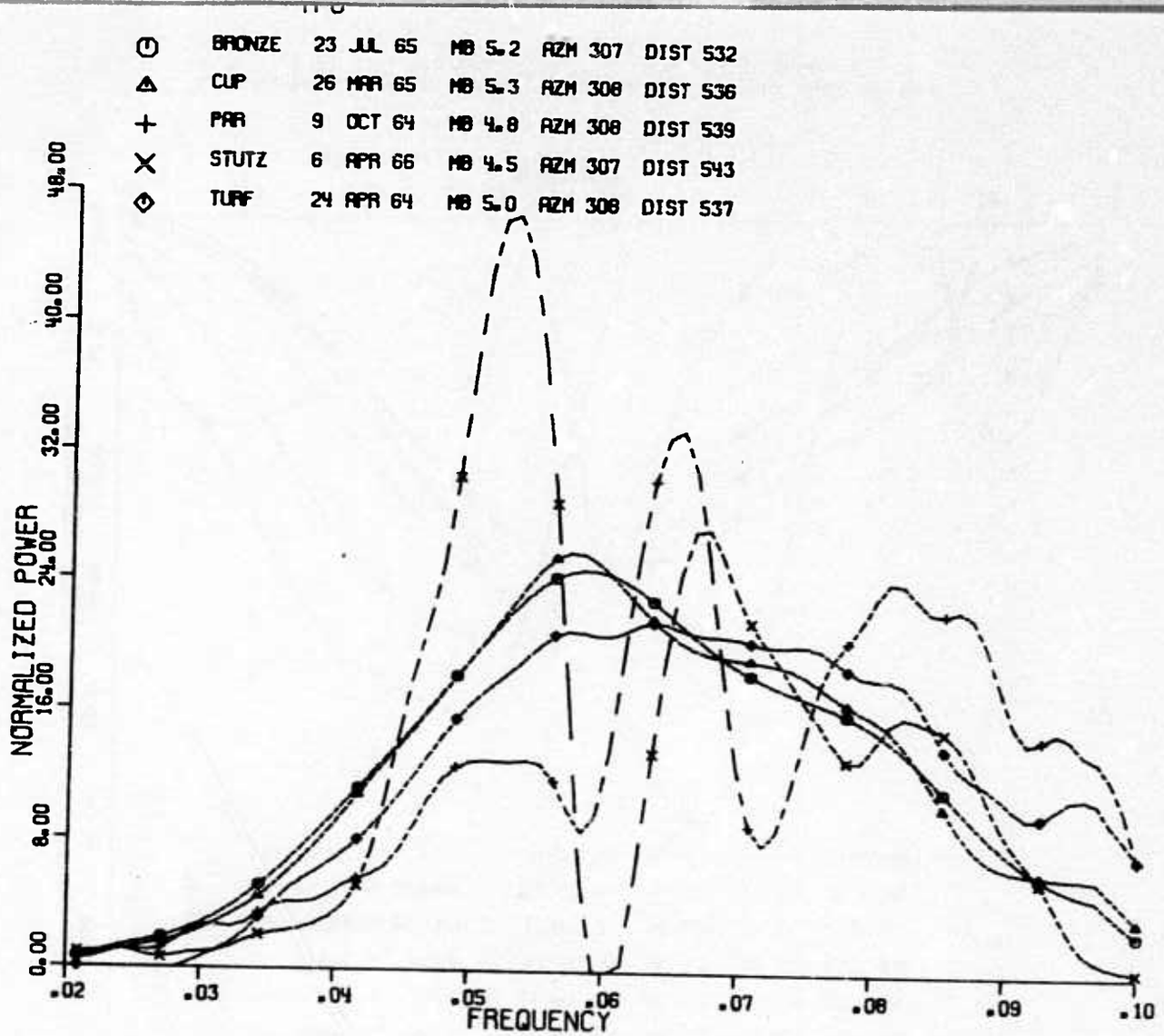

Figure 8. Normalized power spectra for NTS explosions observed at TFO (corrected for instrument response).

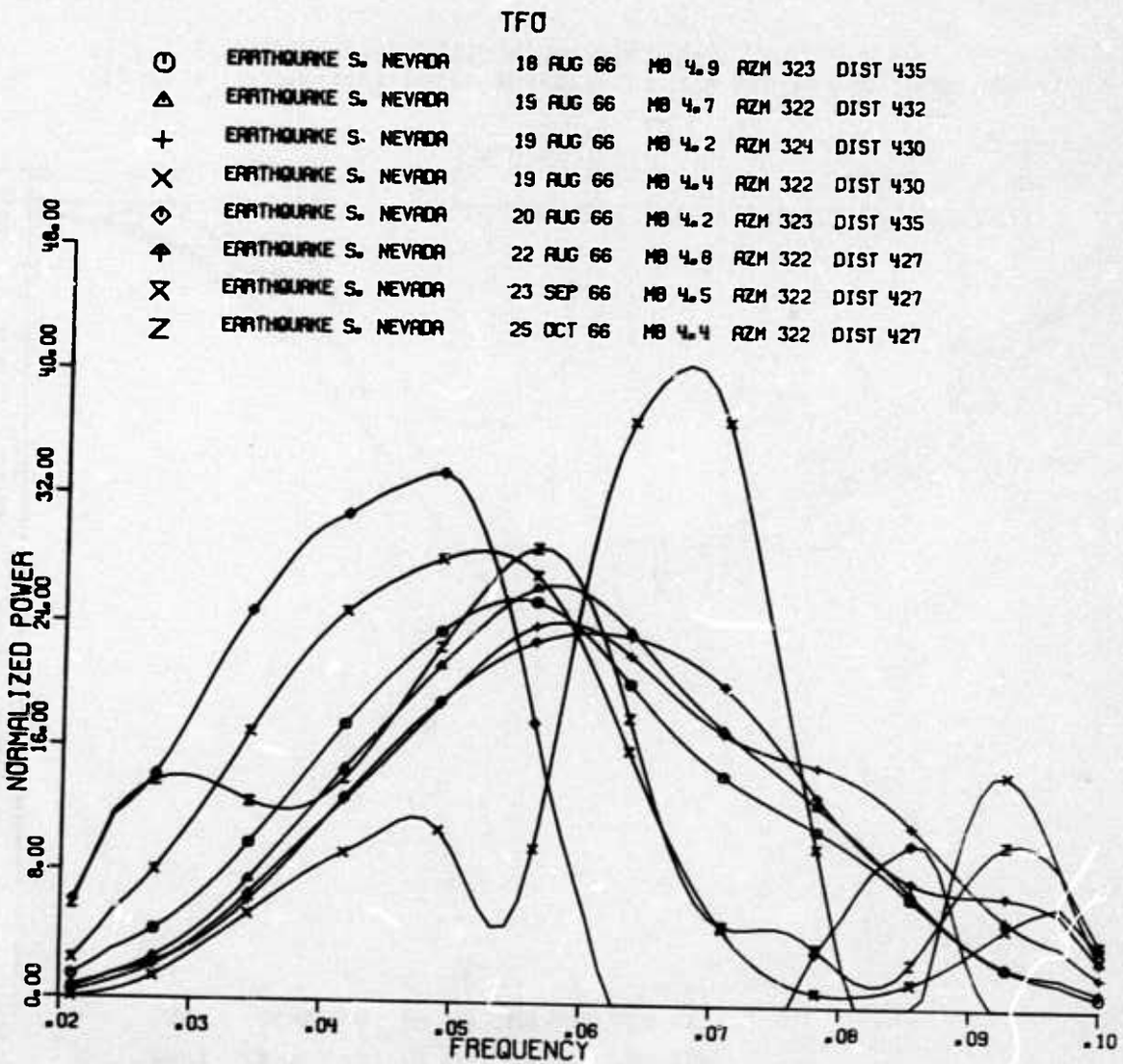

Figure 9. Normalized power spectra for Nevada earthquakes observed at TFO (corrected for instrument response).

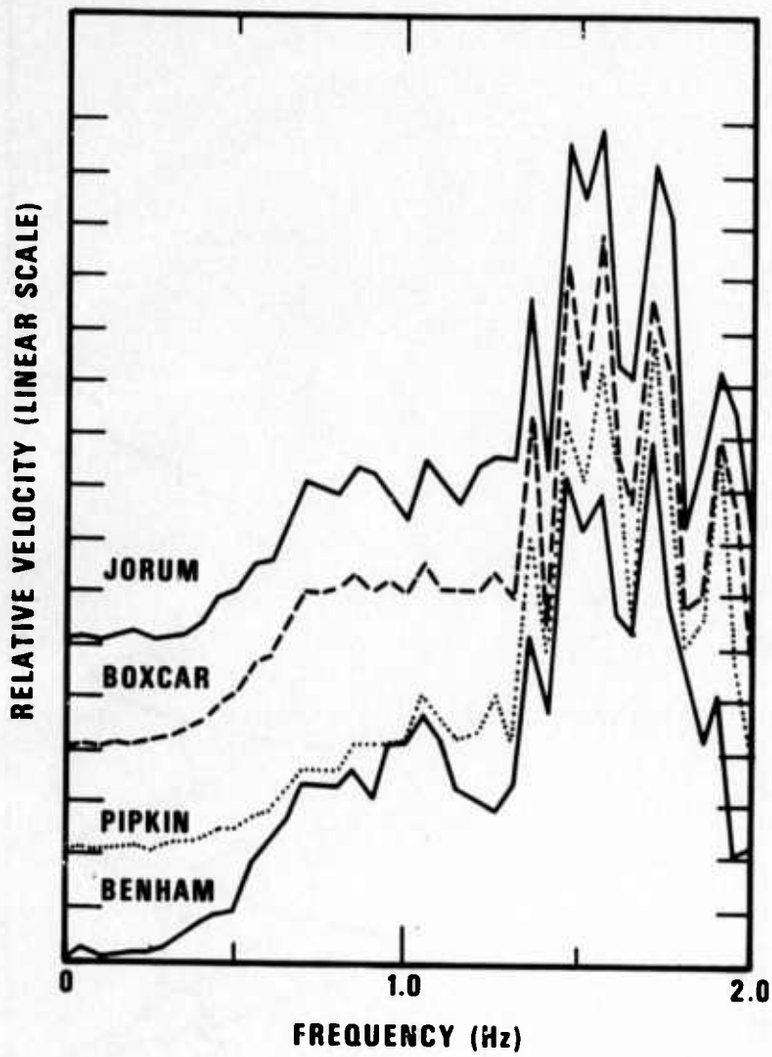

Figure 10. Composite of vertical velocity spectra for four explosions on Pahute Mesa (Jorum, Boxcar, Pipkin, and Benham). Vertical axis gives relative velocity on a linear scale, and each curve has a different absolute scaling value. The curves were so plotted to show clearly the extreme degree of similarity between the spectra of different explosions (from Evernden et al., 1971).

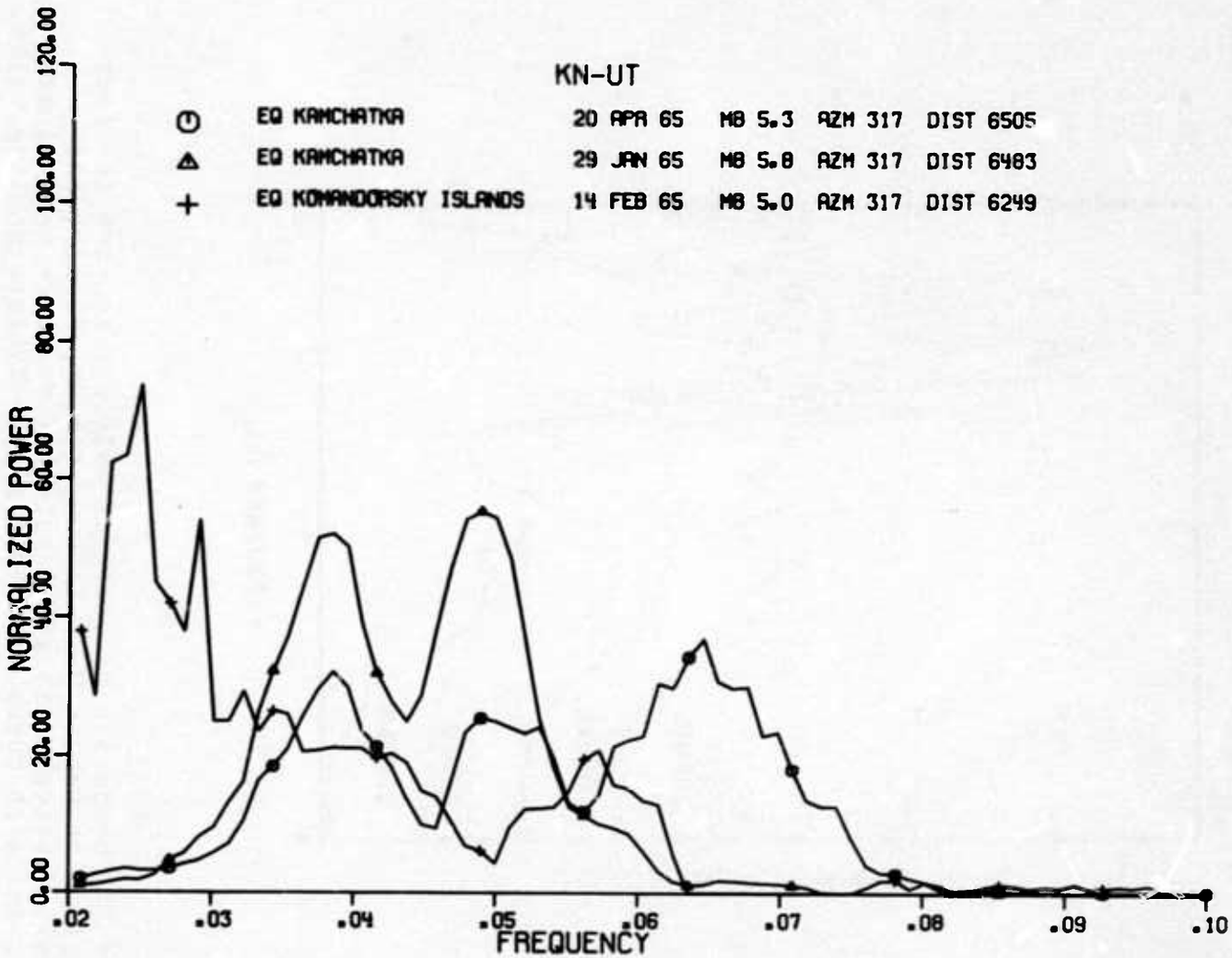

Figure 11. Normalized power spectra for 3 Kamchatka earthquakes observed at KN-UT (corrected for instrument response).

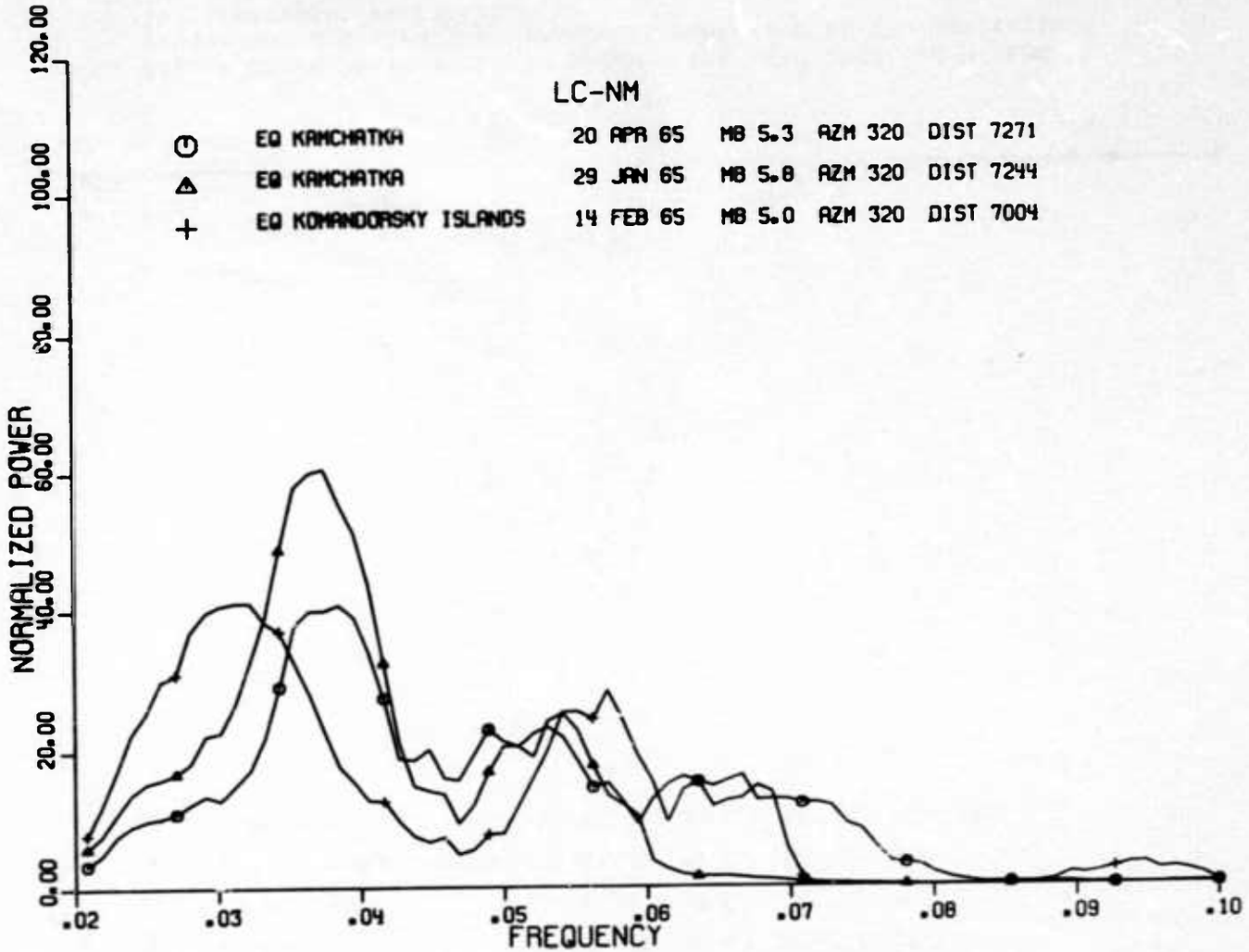

Figure 12. Normalized power spectra for 3 Kamchatka earthquakes observed at LC-NM (corrected for instrument response).

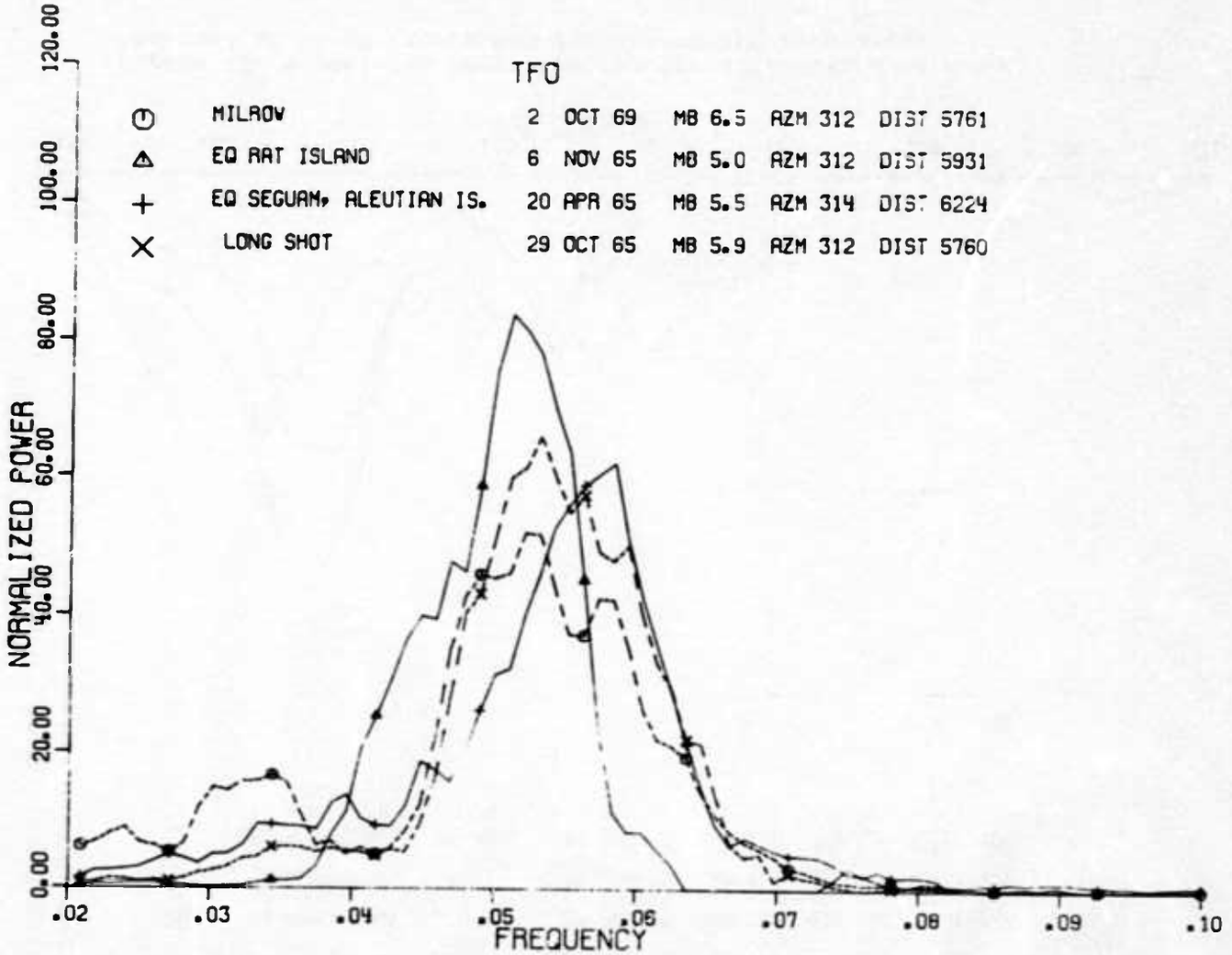

Figure 13. Normalized power spectra for LONG SHOT and MILROW explosions and Aleutian earthquakes observed at TFO (corrected for instrument response).

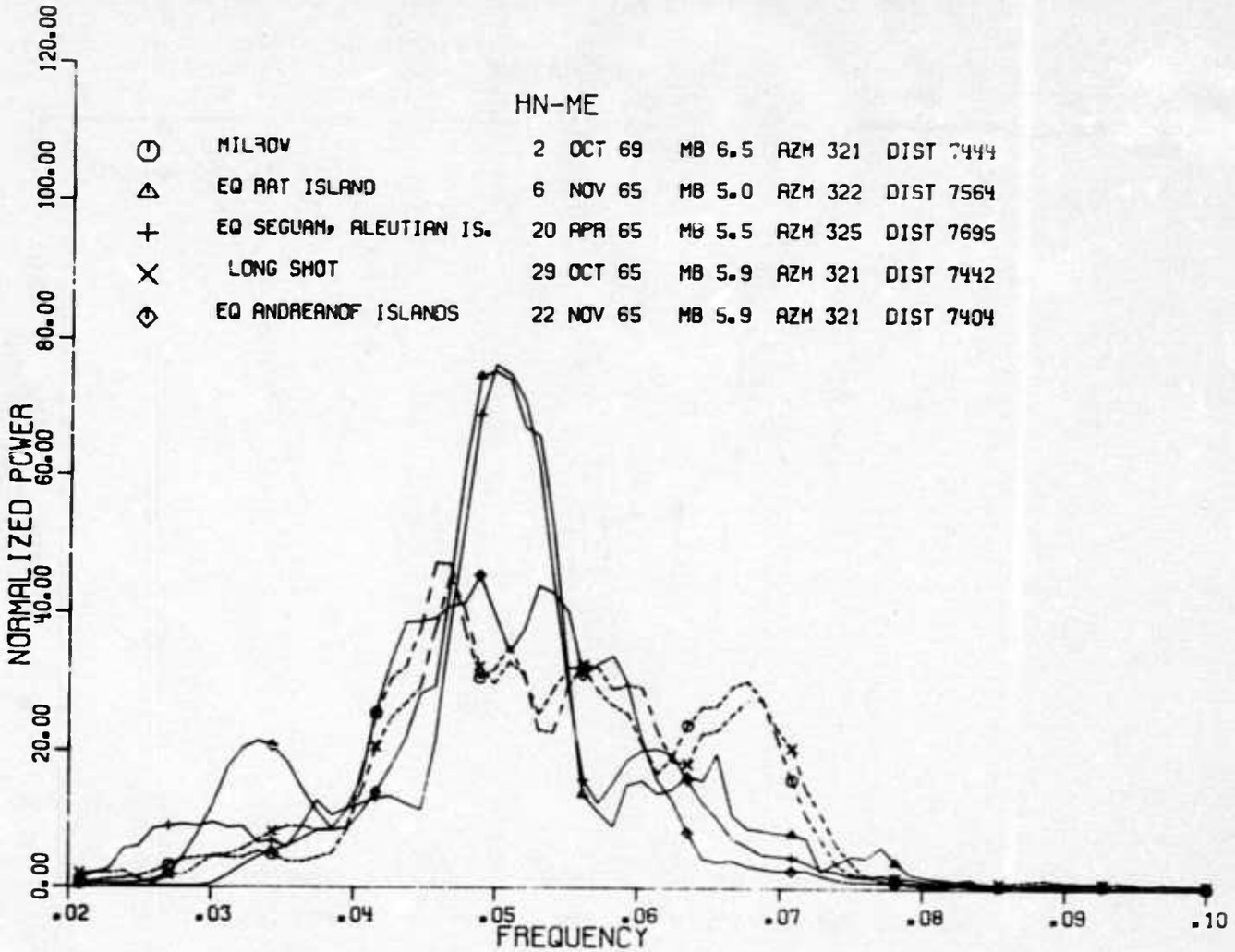

Figure 14. Normalized power spectra for LONG SHOT and MILROW explosions and Aleutian earthquakes observed at HN-ME (corrected for instrument response).

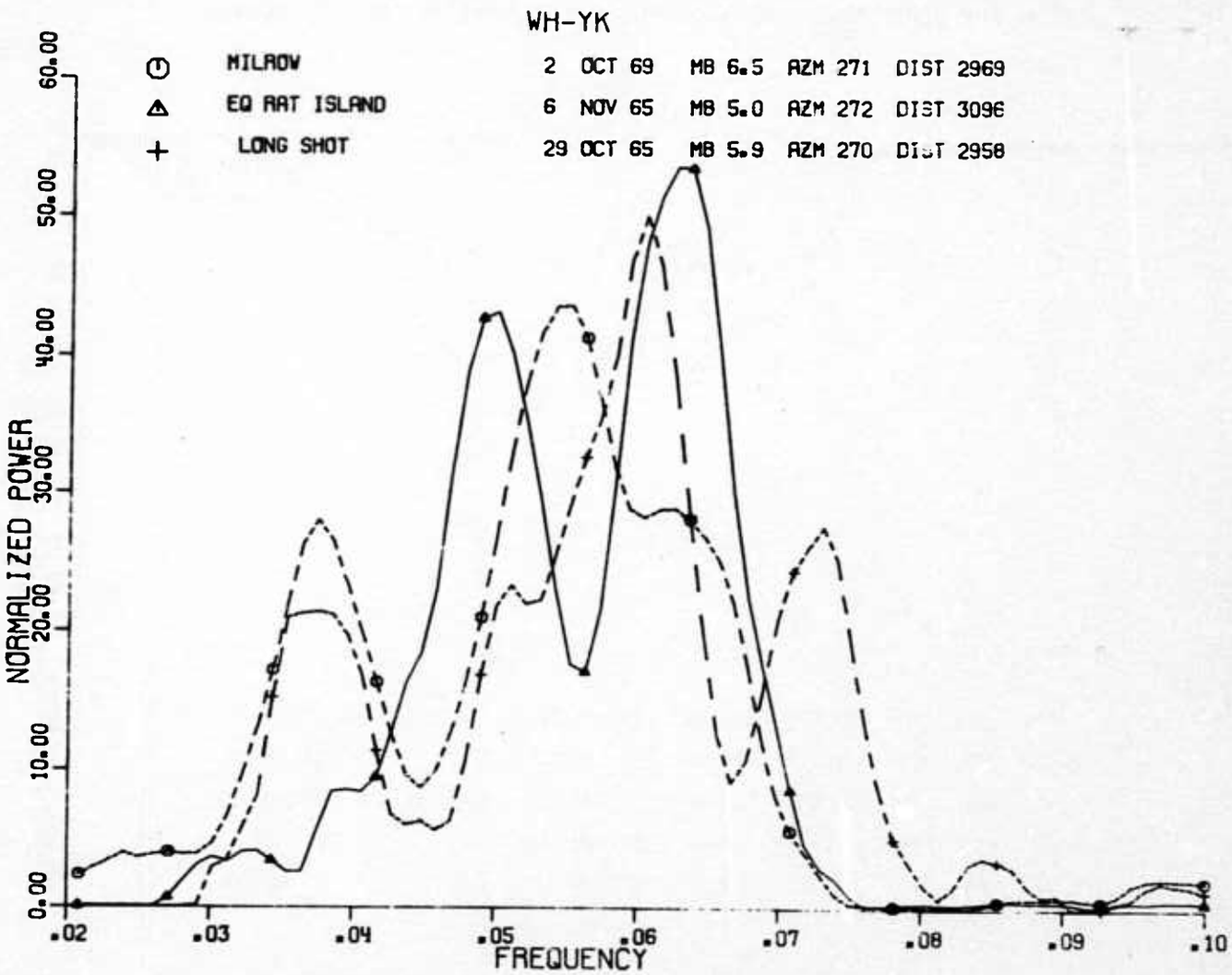

Figure 15. Normalized power spectra for LONG SHOT and MILROW explosions and Aleutian earthquakes observed at WH-YK (corrected for instrument response).

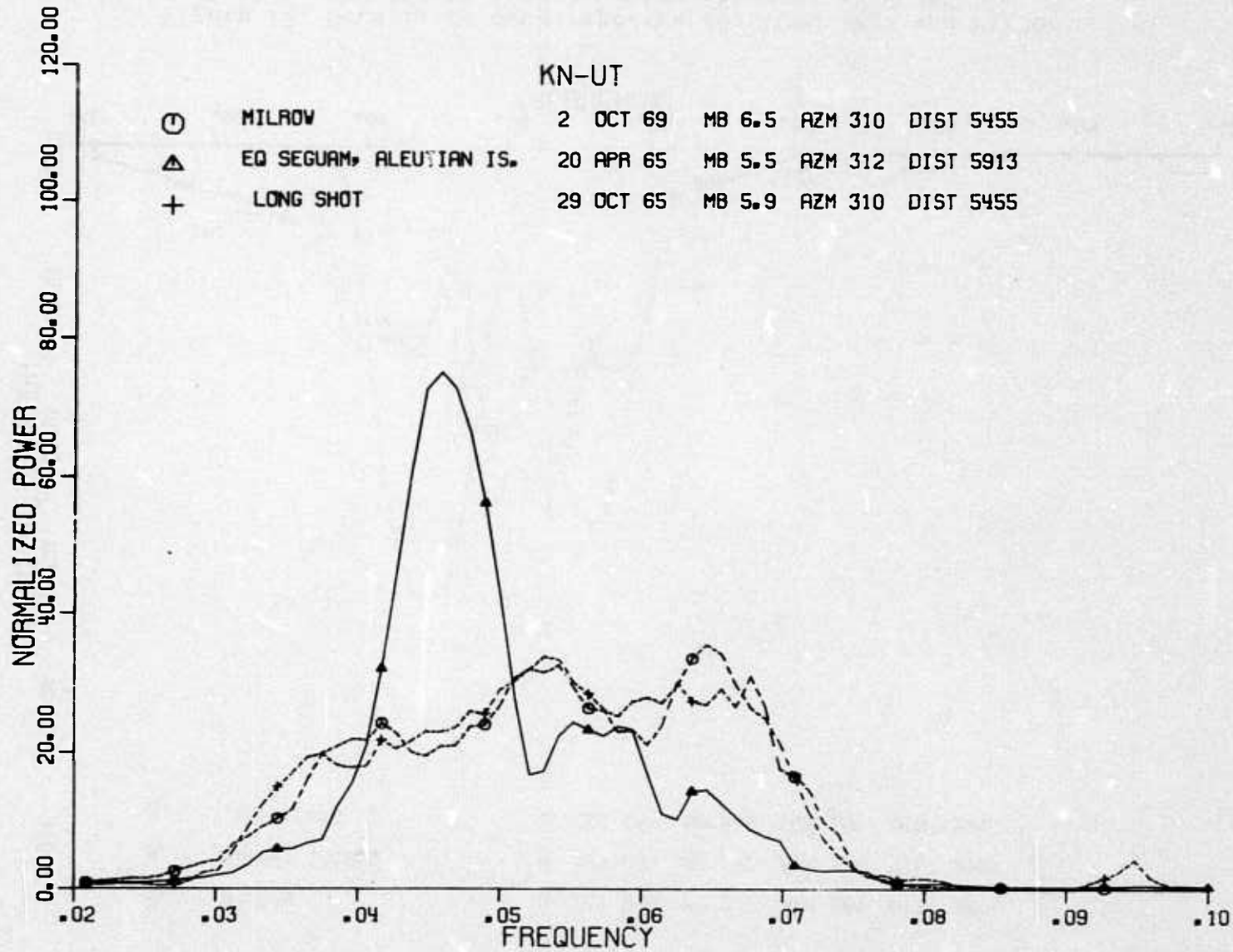

Figure 16. Normalized power spectra for LONG SHOT and MILROW explosions and Aleutian earthquakes observed at KN-UT (corrected for instrument response).

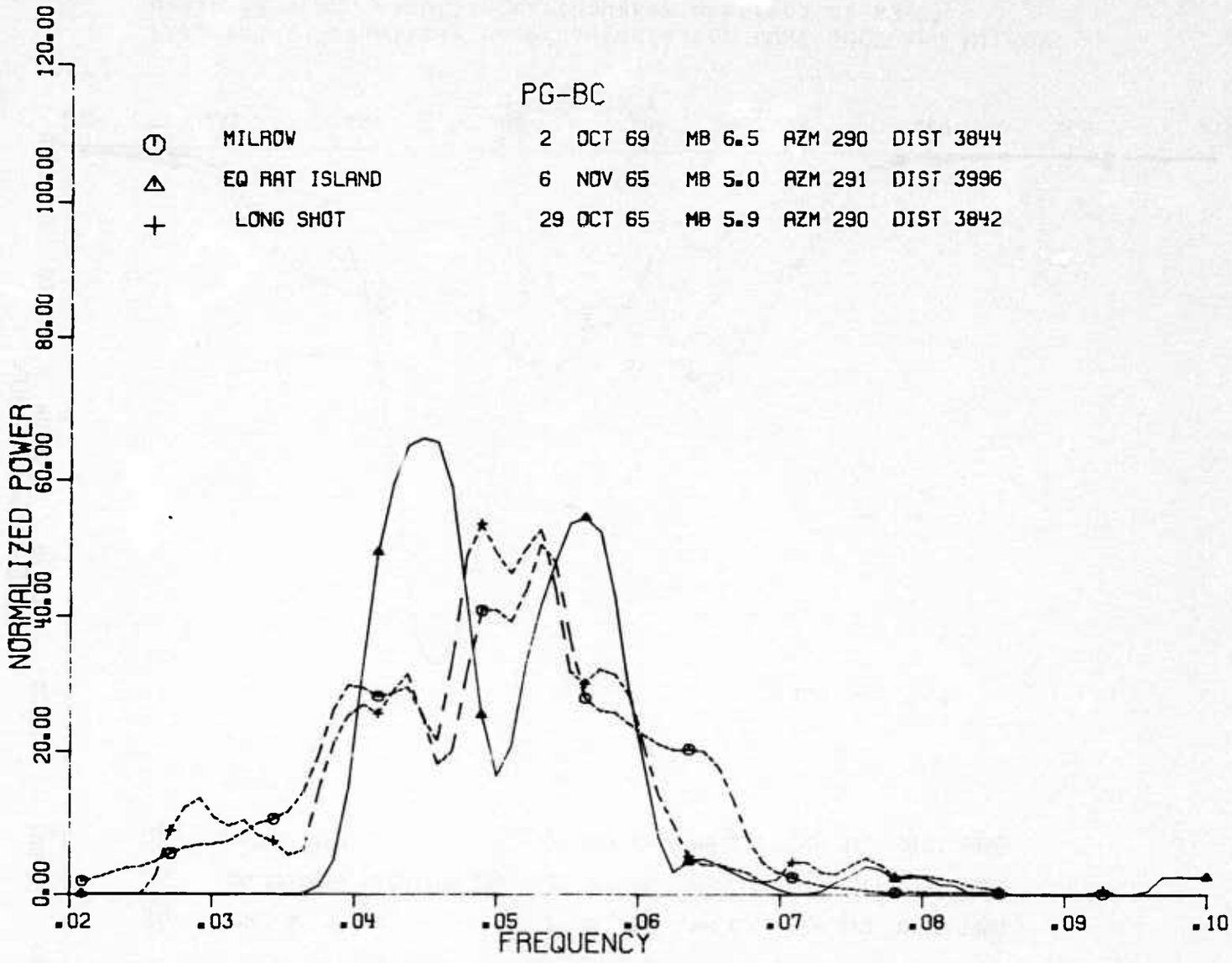

Figure 17. Normalized power spectra for LONG SHOT and MILROW explosions and Aleutian earthquakes observed at PG-BC (corrected for instrument response).

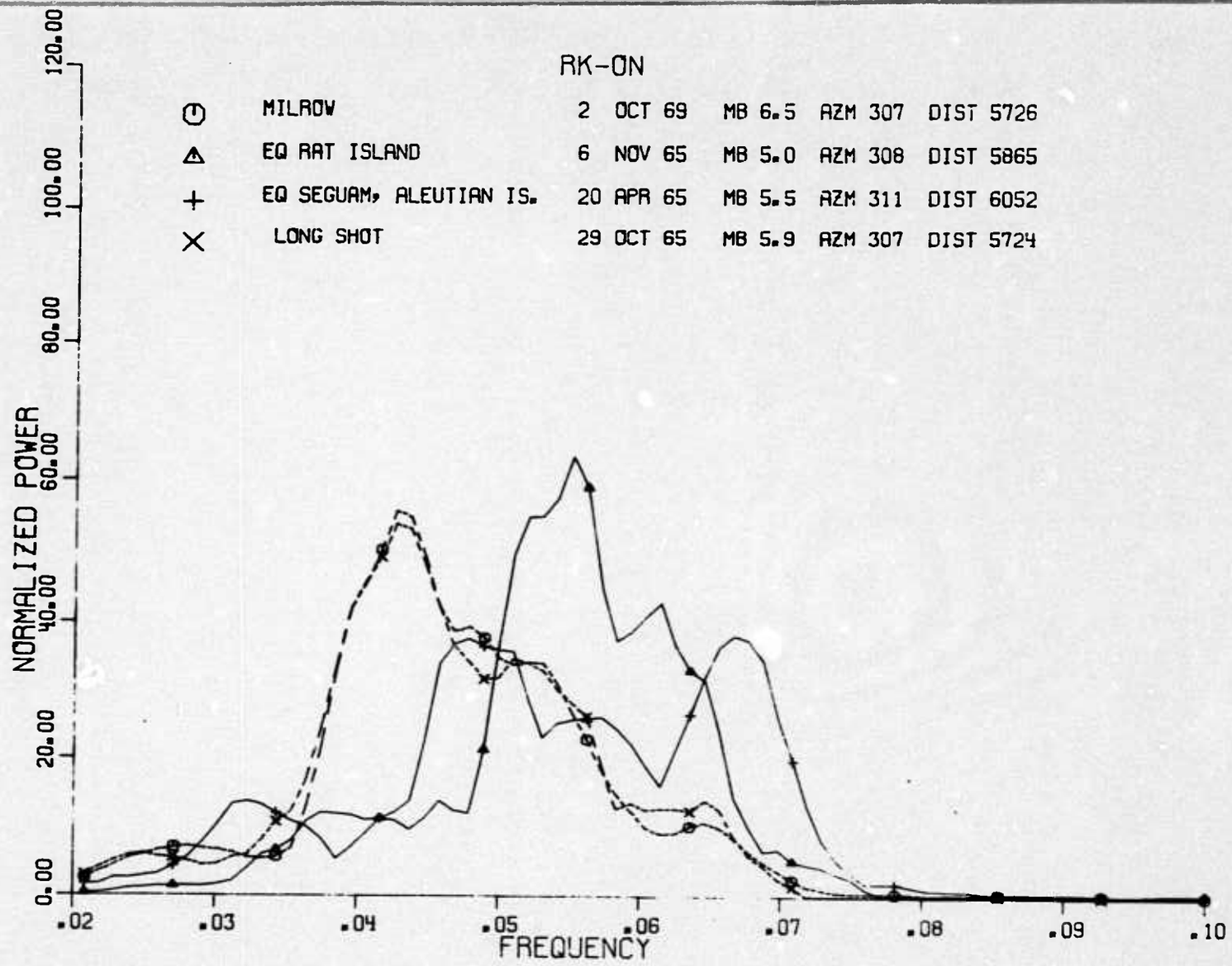

Figure 18. Normalized power spectra for LONG SHOT and MILROW explosions and Aleutian earthquakes observed at RK-ON (corrected for instrument response).